ISBN: 978-3-95450-232-5 ISSN: 2673-7000 doi:10.18429/JACoW-NAPAC2022-TUPA56

BEAM COUPLING IMPEDANCES OF ASYMMETRIC COMPONENTS OF THE SCORPIUS INDUCTION LINAC

S. S. Kurennoy, Los Alamos National Laboratory, Los Alamos, NM, USA

Abstract

The transverse beam coupling impedances of induction linacs must be minimized to avoid beam breakdown instability. The vacuum chamber of the Scorpius linac contains complicated asymmetric elements. We present calculations of the transverse impedances for three asymmetric discontinuities: (1) pumping section between accelerating cells, which contains vacuum plenum, pumping grid, and bellows; (2) fast flapper valve; and (3) debris blocker at the end of the linac. The dipole transverse impedances are calculated with CST Studio using both wake-field solver and eigensolver.

INTRODUCTION

Accelerator vacuum chambers contain multiple discontinuities such as insertions, connections between pieces of beam pipe, pumping holes, etc. The discontinuities contribute to the beam coupling impedances. It is important to make sure that these impedances are acceptable from the viewpoint of beam stability. For small discontinuities, a general analytical method for calculating the impedances was developed in [1]. The beam coupling impedances due to small discontinuities are inductive at low frequencies, i.e., well below the beam-pipe cutoff. Small discontinuities can create trapped modes near the cutoff; they also produce some high-frequency resonances well above the cutoff, at frequencies inversely proportional to discontinuity size.

In more general cases, the beam coupling impedances can be calculated numerically. For calculations of the transverse dipole impedance, which is the most important in induction linacs, asymmetric discontinuities present additional challenges. An approach for impedance calculations in asymmetric cases was first suggested in [2].

The transverse dipole impedance is defined as the ratio of the harmonic of synchronous transverse force induced in the structure to the harmonic of the beam dipole momentum that caused this force [3]. For calculations it is more convenient to use an expression that follows from Panofsky-Wenzel theorem: vertical transverse dipole impedance

$$Z_y(\omega) = cZ_L(\omega, d) / \left(\omega d^2\right), \qquad (1)$$

where $\omega = 2\pi f$, $Z_L(d)$ is the longitudinal impedance calculated along the displaced path (0, d), and d is the vertical displacement from the chamber axis. Similarly, for horizontal dipole impedance Z_x, the field integration path (d, 0) is displaced in x. Equation (1) works for chamber elements with symmetry planes $x = 0$ and/or $y = 0$. For asymmetric elements, the vertical dipole impedance can be found as

$$Z_y(\omega) = \left[d_2 Z_y(d_2) - d_1 Z_y(d_1)\right] / (d_2 - d_1), \qquad (2)$$

which is a weighted difference of two vertical impedances Eq. (1) calculated at different displacements d_1 and d_2 from the beam axis (0, 0, z). The expression for Z_x is similar.

In general, finding impedances from computed wake potentials – time-domain approach [3] – works better for non-resonant or low-Q structures, such as cavities with damping ferrites [4]. For high-Q structures like resonators, it is usually easier to work in frequency domain [3], for example, by calculating eigenmodes.

INTER-CELL PUMPING SECTION

The inter-cell section of the Scorpius induction linac [5] is inserted between two accelerating modules (cells) to provide a connection for a vacuum pump. There are about one hundred such inserts along the linac. The section is a combination of small discontinuities (pumping slots, bellows) with a large asymmetric resonator (vacuum plenum) coupled to the beam pipe by slots. A simplified CST model of inter-cell section is shown in Fig. 1.

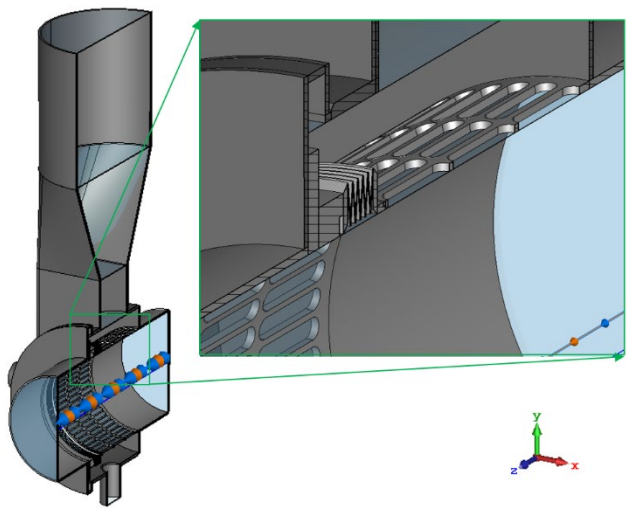

Figure 1: CST model of the inter-cell section: beam pipe, grid with pumping slots, bellows, and vacuum plenum (gray); vacuum volume is shown in transparent blue.

The beam pipe, grid, bellows, and plenum walls are made of stainless steel. The beam pipe and pumping grid both have ID 5.834" (inner radius 74.092 mm) and OD 6"; the grid thickness is 2.108 mm. The vacuum plenum starts as a cylindrical extension that surrounds the pumping grid. It is connected to a duct of rectangular cross section with dimensions 3" x 8", which transitions into a wide cylindrical pipe. There are other elements located nearby, but we will consider the inter-cell section as a single combined discontinuity on a uniform beam pipe.

We use CST wake-field solver to calculate wake potentials due to a Gaussian linear charge distribution with σ_z = 25 mm passing through the inter-cell section up to the distance of s = 25 m behind the bunch. The bunch path is taken on the beam axis ($x = y = 0$) for the longitudinal wake and

ISBN: 978-3-95450-232-5 ISSN: 2673-7000 doi:10.18429/JACoW-NAPAC2022-TUPA56

offset transversely from the axis by distance d, either vertically ($y = d$) or horizontally ($x = d$), for the transverse wake, with proper boundary conditions. The impedances are found as Fourier transforms of the wake potentials normalized by the bunch spectrum [3]. The vertical transverse impedance calculated using Eq. (2) is plotted in Fig. 2.

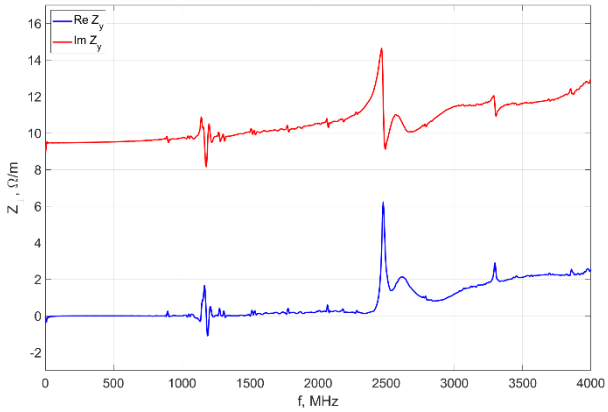

Figure 2: Vertical dipole impedance of the inter-cell section, calculated from wake potentials, versus frequency.

One can see that this impedance is inductive and rather small, which means that the grid screens resonances in the vacuum plenum cavity quite well. There are small peaks corresponding to resonances, mostly near and above the pipe H-mode cutoff, 1186 MHz. If Q-factors of resonances are high, their resonance peaks may not be resolved with wakes calculated to only 25 m. When the length of calculated wake potentials increases, such resonance peaks become higher, while the smooth parts of curves in Fig. 2 remain the same. The best way to evaluate such resonances is with an eigensolver. A few lowest vertical eigenmodes were calculated [6]. The lowest resonance at 892 MHz has Q = 3300 and the resonance impedance R_y = 144 Ω/m, much higher than a tiny peak in Fig. 2. The next two resonances are at 1050 and 1150 MHz; they have Q-values 4700 and 950 with R_y of 130 and 140 Ω/m, respectively. The first two resonances are due to vacuum-plenum modes, the third one is produced by a trapped mode slightly below the pipe cutoff frequency; see in [3].

The behavior of the horizontal dipole impedance is similar, though the resonance impedances are lower, with the largest value of 17 Ω/m. More details and pictures of resonance fields can be found in report [6].

TRANSPORT LINE ELEMENTS

The following two elements are installed after the Scorpius linac, in the beam transport line. Unlike inter-cell sections, which are inserted between all linac cells, both are single elements. Still their impedances should be evaluated to ensure beam stability.

Fast Flapper Valve

The fast flapper valve serves to prevent target debris from penetrating into the linac. A CAD model of fast valve was imported into CST and simplified as shown in Fig. 3. The valve is asymmetric in the horizontal direction.

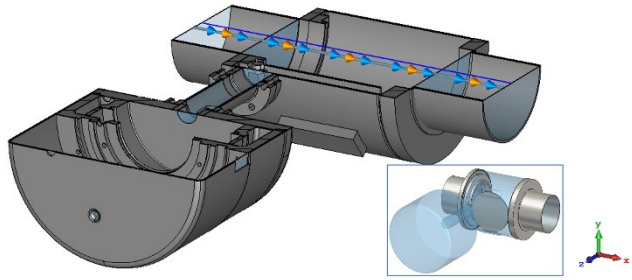

Figure 3: CST model of fast valve for wake calculations, cut horizontally. Inset shows an eigensolver model. Stainless steel is in gray, vacuum volume in transparent blue.

The valve impedances were first calculated from wake potentials up to s = 25 m, see Fig. 4, which indicated frequencies of high-Q resonances. For horizontal dipole impedance, two wake potentials with different displacements were computed and Eq. (2) was applied.

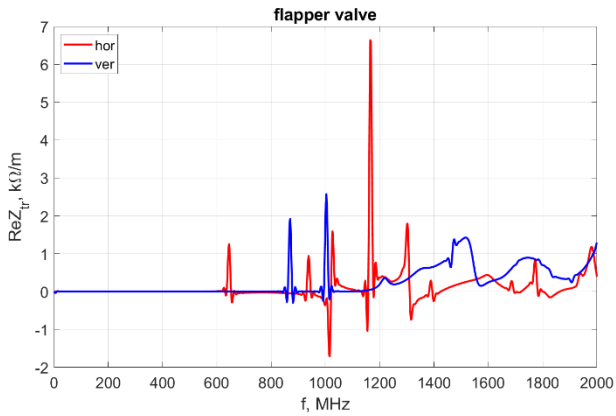

Figure 4: Transverse dipole impedances of the fast valve from wake potentials with s = 25 m, versus frequency.

Further computations with longer wakes, up to the distance of s = 500 m, showed that the resonance peak heights increase for longer wakes. More accurate evaluation of resonances was performed with eigensolver. The lowest vertical transverse modes are at 873 and 1005 MHz, with Q-values 700 and 2160 and shunt impedances R_v of 17.7 and 69.2 kΩ/m, respectively. Two lowest horizontal modes are at 645 and 938 MHz. They have even higher impedances, R_h = 295 kΩ/m and 834 kΩ/m, with Q = 330 and 3960. The strange negative peak near 1021 MHz was identified as a mixed, mostly longitudinal, mode, see in Fig. 5.

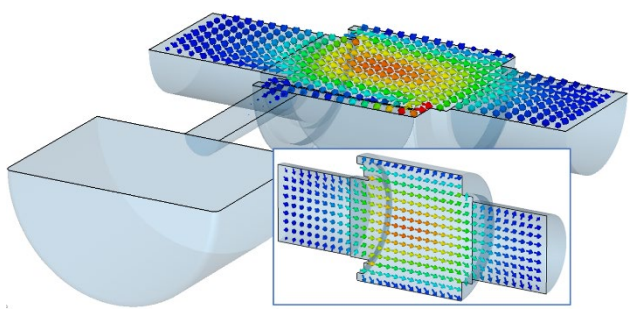

Figure 5: Electric field of the mixed mode at 1021 MHz.

ISBN: 978-3-95450-232-5 ISSN: 2673-7000 doi:10.18429/JACoW-NAPAC2022-TUPA56

Debris Blocker

The debris blocker consists of two rotating metal disks with cuts, which provide an opening for a beam pulse when the cuts overlap. It protects the linac from target debris. A CAD model was imported into CST and simplified as shown in Fig. 6. The valve is asymmetric in the horizontal direction (w.r.t. the vertical plane $x = 0$) since the two disks are separated by a short distance along the beam path.

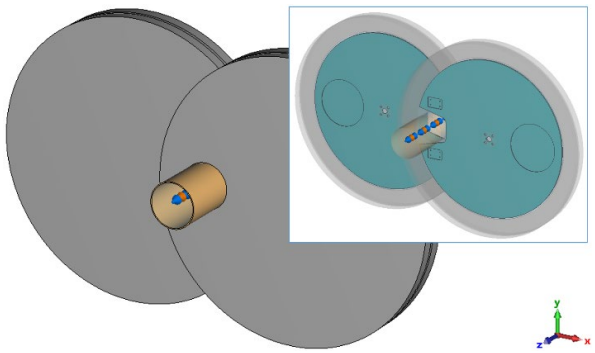

Figure 6: CST model of debris blocker for wake calculations, cut horizontally. Inset shows metal disks with cuts.

We used a modified method to calculate the dipole transverse impedance in the asymmetric direction [7]. We run two parallel Gaussian beams with the same charge distribution but opposite charges (q and $-q$) at transverse displacements $x = d$ and $x = -d$ from the axis. Transverse wake potentials produced by both beams along a given path (e.g., following one beam, $x = d$) were calculated. Combining their impedance contributions gives the transverse dipole impedance, like Eq. (2). This method gives the same results as Eq. (2); it was checked for the debris blocker, as well as for the inter-cell section described above.

The real part of the transverse dipole beam coupling impedances of the debris blocker calculated from wake potentials is plotted in Fig. 7. Both impedances exhibit narrow resonance peaks above 400 MHz, which correspond to resonances in two shallow cavities surrounding disks.

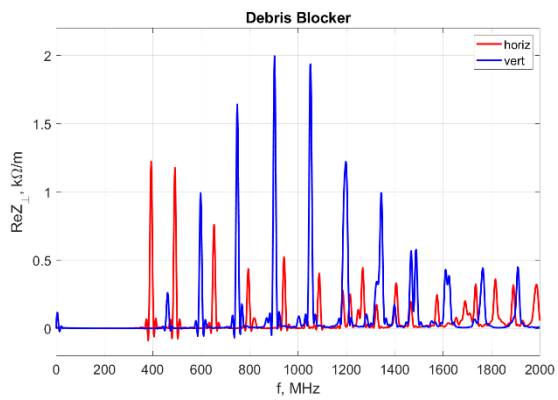

Figure 7: Transverse dipole impedances of debris blocker.

At frequencies below the resonances, the imaginary part of transverse impedance is inductive and nearly constant: $|\mathrm{Im}\, Z_x| = 160\ \Omega/\mathrm{m}$, $|\mathrm{Im}\, Z_y| = 180\ \Omega/\mathrm{m}$. The CST eigensolver was used to identify the modes in Fig. 7. Using one-half geometry with the electric boundary in the horizontal plane, we found 30 vertical modes below 1 GHz. For the full geometry, there are 60 modes below 1 GHz, which include both transverse and vertical ones, as well as other modes that may or may not contribute to the transverse impedance. All eigenmodes come in pairs – two modes having very close frequencies – because we have two practically identical short cavities housing the disks that are weakly coupled through the beam pipe. The Q values slowly increase with the mode number, but all Qs are rather small – from about 60 for the lowest modes to below 200 for the highest modes calculated. This is because of large surface losses in the short flat disk cavities with steel walls: the ratio of cavity volume to its surface area is proportional to the cavity length and quite small. As a result, some peaks in Fig. 7 are formed by two overlapping modes. More details and mode fields can be found in Tech Note [7].

CONCLUSION

The transverse beam coupling impedances of asymmetric discontinuities in the Scorpius linac are calculated. The impedances of inter-cell pumping inserts are small. For the fast valve and debris blocker the maximal impedances exceed those of the Scorpius accelerator cells, which are below 700 Ω/m [4]. However, there will be 102 accelerator cells along the linac, compared to such single elements at its end. Therefore, we can conclude that the impedances of these elements are not dangerous from the viewpoint of linac beam stability.

ACKNOWLEDGEMENTS

The author acknowledges useful discussions with many LANL colleagues, but especially with C.A. Ekdahl, R.C. McCrady, and G.E. Dale.

REFERENCES

[1] S. S. Kurennoy, R.L. Gluckstern, and G.V. Stupakov, "Coupling impedances of small discontinuities: a general approach", *Phys. Rev. E*, v. 52, p. 4354, 1995. doi:10.1103/PhysRevE.52.4354

[2] S. Heifets, A. Wagner, and B. Zotter, "Generalized impedances and wakes in asymmetric structures", Report SLAC/AP110, 1998.

[3] "Impedances and Wake Functions", in *Handbook of Accelerator Physics and Engineering*, Eds. A.W. Chao *et al.*, 2nd Ed., World Sci., 2013, Sec. 3.2.

[4] S. S. Kurennoy and R. C. McCrady, "Beam Coupling Impedances of Ferrite-Loaded Cavities: Calculations and Measurements", in *Proc. IPAC'21*, Campinas, Brazil, May 2021, pp. 696-699. doi:10.18429/JACoW-IPAC2021-MOPAB211

[5] M. Crawford and J. Barraza, "Scorpius: The development of a new multi-pulse radiographic system," in *Proc. IEEE 21st Int. Conf. Pulsed Power*, Brighton, U.K., pp. 1–6, 2017.

[6] S. S. Kurennoy, "Coupling impedances of inter-cell section in Scorpius linac," LA-UR-21-32382, Los Alamos, 2021.

[7] S. S. Kurennoy, "Transverse Beam Coupling Impedances of Scorpius Debris Blocker," Tech Note AOT-AE: 21-005, Los Alamos, 2021.